

## Diffusion behavior and distribution regulation of MgO in MgO-bearing pellets

Qiang-jian Gao<sup>1)</sup>, Yan-song Shen<sup>2)</sup>, Guo Wei<sup>1)</sup>, Xin Jiang<sup>1)</sup>, and Feng-man Shen<sup>1)</sup>

1) School of Metallurgy, Northeastern University, Shenyang 110819, China

2) School of Chemical Engineering, University of New South Wales, NSW 2052, Australia

(Received: 12 December 2015; revised: 25 May 2016; accepted: 30 May 2016)

**Abstract:** In this paper, the diffusion behavior between MgO and Fe<sub>2</sub>O<sub>3</sub> (the main iron oxide in pellets) is investigated using a diffusion couple method. In addition, the distribution regulation of MgO in MgO-bearing pellets is analyzed via pelletizing experiments. The results illustrate that MgO is prone to diffuse into Fe<sub>2</sub>O<sub>3</sub> in the form of solid solution; the diffusion rate considered here is 13.64 μm·min<sup>-1</sup>. Most MgO content distributes in the iron phase instead of the slag phase. The MF phase {(Mg<sub>1-x</sub>Fe<sub>x</sub>)O·Fe<sub>2</sub>O<sub>3</sub>, x ≤ 1} is generated in the MgO-bearing pellets. However, the distribution of MgO in the radial direction of the pellets is inconsistent. The solid solution portion of MgO in the MF phase is larger in the outer layer of the pellets than in the inner layer. In this work, the approximate chemical composition of the MF phase in the outer layer of the pellets is {(Mg<sub>0.35-0.77</sub>Fe<sub>0.65-0.23</sub>)O·Fe<sub>2</sub>O<sub>3</sub>} and in the inner layer is {(Mg<sub>0.13-0.45</sub>Fe<sub>0.87-0.55</sub>)O·Fe<sub>2</sub>O<sub>3</sub>}.

**Keywords:** magnesia; iron oxide; ore pellets; diffusion; distribution

### 1. Introduction

Acid pellets, the traditional iron-bearing burden materials for blast furnace (BF) [1], have many advantages in terms of their intrinsic and metallurgical properties [2–4]: better mechanical strength, which is favorable for transportation and storage; relatively uniform particle size distribution, favorable for burden permeability in BFs; high iron-grade, favorable for effective iron content input into the burden column and for enhancing the production efficiency of BFs [5–6]; etc. Therefore, the proportion of acid pellets used as burden materials is increasing, 20wt% in China and even 100wt% in parts of Europe and North America.

However, when acid pellets are reduced in BFs, FeO and SiO<sub>2</sub> display high reaction rates, forming the low melting point mineral fayalite [7]. Consequently, the softening/melting properties of the pellets deteriorate, leading to lower permeability in the cohesive zone and limited indirect reduction [8–10]. Reduction swelling of acid pellets is also another limit on their use in BFs. In order to improve their high-temperature metallurgical properties it is possible to introduce fluxes into the pellets. For example, a CaO-bearing

flux can be added to produce self-fluxing pellets for improvement in the softening and melting properties. Nevertheless, reduction swelling is still evident and these cannot be used in BFs on a large scale [11]. Alternatively, an MgO-bearing flux can be added to the pellets. Many beneficial effects of MgO addition during the reduction process have been summarized in previous studies [12–13]. The most essential benefit is an increase in the high-temperature properties of the pellets due to the solution of MgO in wustite and slag. This results in favorable cohesive zone configuration, reasonable gas distribution, and increase in productivity [14–17], as well as meeting the slagging requirements of MgO.

As with ordinary acid pellets, the induration process of MgO-bearing pellets is accomplished in the solid phase (different from iron ore sinter which is agglomerated by the binding phase), which includes the recrystallization of Fe<sub>2</sub>O<sub>3</sub> and solid solution of MgO [18–19]. Therefore, adequate diffusion and reaction of MgO in pellets is essential for its efficient and economical use. From the literatures, the effects of MgO on agglomeration (sintering and pelletizing) can be summarized as follows. Semberg *et al.* [20] showed that when adding MgO (as fine olivine with particle size

Corresponding author: Feng-man Shen E-mail: gaoqiangjian@163.com

© University of Science and Technology Beijing and Springer-Verlag Berlin Heidelberg 2016

<38  $\mu\text{m}$ ) to pellets, the whole magnesium content of the olivine is evenly dissolved in the wustite, and the pellet strength is restrained. Similarly, a previous paper [21], maintained that the pellet strength depends on the diffusion and solid solution of MgO into the pellets. Moreover, Singh and Björkman [22] demonstrated that the solid solution reaction between MgO and FeO can be achieved with less resistance during the sintering process. On the basis of the above, it is acknowledged that an appropriate MgO content in pellets improves the metallurgical properties. However, MgO diffusion behavior in pellets has been reported rarely and further studies are essential. Detailed studies on the diffusion behavior of MgO in pellets are fundamental to the efficient use of MgO resources. In this work, the diffusion behavior of MgO in  $\text{Fe}_2\text{O}_3$  was investigated using diffusion couple experiments. Furthermore, the distribution and migration of MgO in the pellets was analyzed using pelletizing experiments.

## 2. Experimental

### 2.1. Experiment preparation

The raw materials included pure reagents (MgO and  $\text{Fe}_2\text{O}_3$ ) for the diffusion couple experiments, and calcined magnesite, bentonite, and magnetite for the pelletizing experiments. The chemical composition is listed in Table 1.

**Table 1. Chemical composition of raw materials** wt%

Raw materials	TFe	MgO	$\text{SiO}_2$	$\text{Al}_2\text{O}_3$	$\text{K}_2\text{O} + \text{Na}_2\text{O}$	LOI
Magnetite	64.5	0.14	6.07	0.12	—	1.36
Calcined magnesite	—	83.50	5.11	0.72	—	8.32
Bentonite	1.93	—	60.89	19.65	4.45	12.21

Note: LOI — loss on ignition.

### 2.2. Method and procedure

#### 2.2.1. Diffusion behavior of MgO in $\text{Fe}_2\text{O}_3$

Detailed studies on MgO diffusion behavior were carried out via diffusion couple experiments. MgO and  $\text{Fe}_2\text{O}_3$  reagents (particle size:  $-74 \mu\text{m} > 95\%$ ) were used to prepare MgO– $\text{Fe}_2\text{O}_3$  diffusion couples. The samples were prepared in a mold and maintained at a pressure of 100 MPa for 5 min. The samples are thin enough to minimize the influence of temperature difference on the diffusion between MgO and  $\text{Fe}_2\text{O}_3$ . The thickness of the MgO and  $\text{Fe}_2\text{O}_3$  samples was 1 mm and the diameter was 10 mm. A general view of a sample is shown in Fig. 1.

After preparation, the MgO– $\text{Fe}_2\text{O}_3$  diffusion couples were put into an electronic furnace preheated at  $900^\circ\text{C}$ , the

temperature was then increased to  $1250^\circ\text{C}$ , and finally held at  $1250^\circ\text{C}$  for 20 min. The details of heating process, designed according to the induration process of iron ore pellets, are shown in Fig. 2. The samples, packaged in epoxy resin, were cut along the diffusion direction, and the diffusion behavior between the FeO and MgO was analyzed using a scanning electron microscope (SEM).

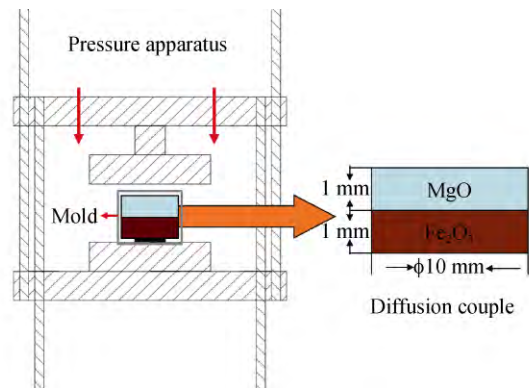


**Fig. 1. MgO and  $\text{Fe}_2\text{O}_3$  diffusion couple.**

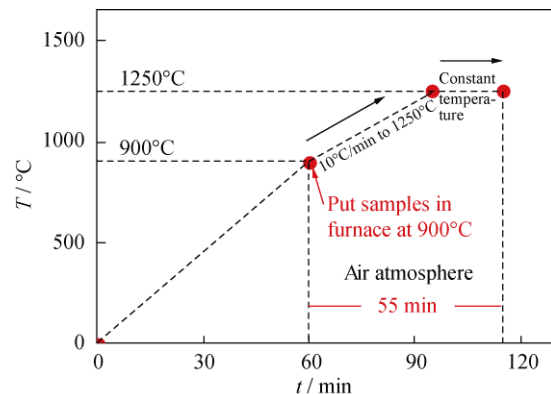


**Fig. 2. Heating system parameters.**

#### 2.2.2. Distribution behavior of MgO in pellets

The distribution and migration of MgO in pellets was investigated based on pelletizing experiments in the laboratory. The pelletizing process is summarized in the following steps. (1) Green pellets. In this step, the main parameters included an  $8.0\% \pm 0.5\%$  moisture content and a 30 min pelletizing time. (2) Drying. The green pellets in this step were dried at  $105^\circ\text{C}$ . (3) Induration. The dried pellets were indurated in a muffle furnace preheated at  $900^\circ\text{C}$ ; air was blasted into the furnace at a flow-rate of 1.2 L/min. The furnace temperature was increased to  $1250^\circ\text{C}$  over a period of 35 min, and then the pellets were roasted for 20 min. After the pelletizing process, the ordinary acid pellets (no MgO) and the MgO-bearing pellets (mass fraction 4.0wt% MgO) were polished and scanned with the SEM, and the distribution of MgO in the pellets was analyzed using an energy dispersive

X-ray detector (EDX).

### 2.3. Reproducible experiment

Reproducible experiments were carried out to improve accuracy of the results. Both the diffusion experiments and pelletizing experiments were repeated twice. The arithmetic mean of the two results was then used as the final result.

## 3. Diffusion behavior of MgO in Fe<sub>2</sub>O<sub>3</sub>

### 3.1. Diffusion mechanism

It is well-known that solid phase reaction is caused by ion diffusion [11]. Generally, in a solid phase reaction that generates a complex compound between the two kinds of oxide, the reaction temperature range is usually wide. Therefore, the reaction rate is slower as the temperature is lower. Contrarily, it is easier for diffusion to occur when the temperature is high. Actually, during the induration process, the MgO and Fe<sub>2</sub>O<sub>3</sub> reaction is also a solid phase reaction. Two routes are proposed for the mass-transfer behavior of the reaction ( $\text{MgO} + \text{Fe}_2\text{O}_3 = \text{MgFe}_2\text{O}_4$ ), as shown in Fig. 3. As the active ions are  $\text{Mg}^{2+}$  and  $\text{O}^{2-}$ , they first migrate to the boundary ( $\text{MgFe}_2\text{O}_4\text{-Fe}_2\text{O}_3$ ), and react with Fe<sub>2</sub>O<sub>3</sub> (Fig. 3(a)); similarly, if the active ions are  $\text{Fe}^{3+}$  and  $\text{O}^{2-}$ , they

move to the  $\text{MgFe}_2\text{O}_4\text{-MgO}$  boundary and fulfill the following reaction (Fig. 3(b)).

Cross-sections of the MgO-Fe<sub>2</sub>O<sub>3</sub> diffusion couples, analyzed by SEM, are shown in Fig. 4. On the basis of various gray levels, different layers are evident from left to right in Fig. 4(a), i.e., MgO layer (dark gray), diffusion reaction layer (grayish), Fe<sub>2</sub>O<sub>3</sub> layer (white), and resin (black). Fig. 4(b) shows the microstructure of the reaction interface labeled as “point b” in Fig. 4(a). Similarly, the leading edge of the diffusion reaction is shown in Fig. 4(c). From Fig.4, it can be concluded that Fe<sub>2</sub>O<sub>3</sub> rarely occurs in the MgO layer. However, the Fe<sub>2</sub>O<sub>3</sub> layer diminishes gradually as most of it is substituted by the diffusion reaction layer. MgO is inclined to diffuse into Fe<sub>2</sub>O<sub>3</sub>.

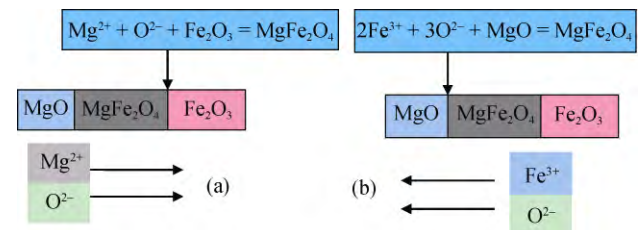


Fig. 3. Mass-transfer diagram of the reaction  $\text{MgO} + \text{Fe}_2\text{O}_3 = \text{MgFe}_2\text{O}_4$ : (a) active ions are  $\text{Mg}^{2+}$  and  $\text{O}^{2-}$ ; (b) active ions are  $\text{Fe}^{3+}$  and  $\text{O}^{2-}$ .

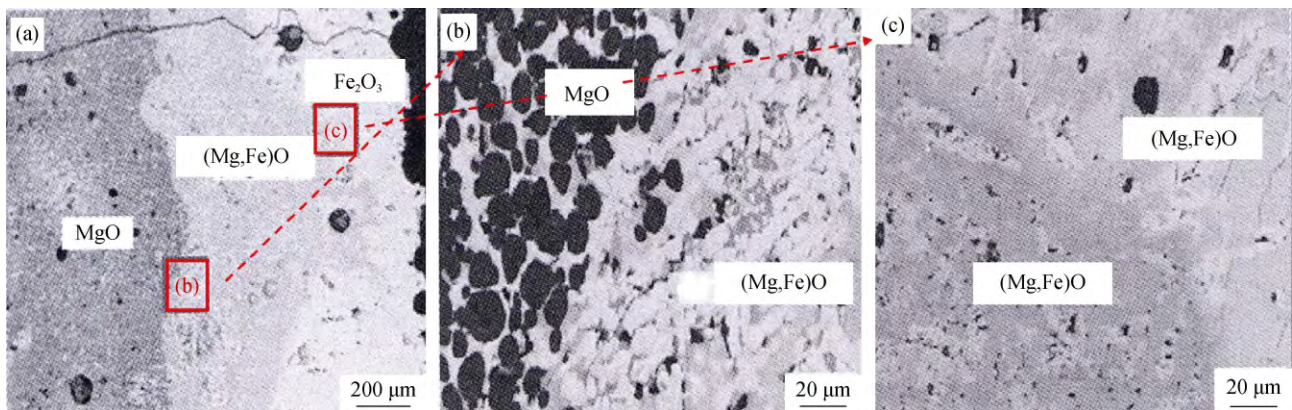


Fig. 4. SEM photographs of the diffusion process between Fe<sub>2</sub>O<sub>3</sub> and MgO: (a) cross section of the diffusion couple; (b) reaction interface; (c) reaction leading edge.

### 3.2. Diffusion rate

The thickness of the diffusion layer was determined with SEM photographs of sample cross-sections. The diffusion layer was divided into 24 sections ( $\Delta H$ ) mostly in a perpendicular direction. The thickness of each section is denoted as  $L_1, L_2, L_3, \dots, L_{25}$  (Fig. 5) and the thickness of the diffusion layer ( $L$ ) is calculated using Eq. (1).

$$L = \frac{L_1 + L_2 + \dots + L_{25}}{25} \quad (1)$$

Based on Fig. 5, the conclusion is drawn that the diffusion layer thickness can be increased gradually by prolonging the reaction time at 1250°C. According to the method mentioned above,  $L$  can be calculated at different reaction times, as listed in Table 2.

The relationship between diffusion layer thickness ( $L$ ) and time ( $t$ ) is shown in Fig. 6.

Linear fitting is listed in Eq. (2).

$$L = 13.64 t + 90.87 \quad (2)$$

The diffusion rate can be obtained from Eq. (3)

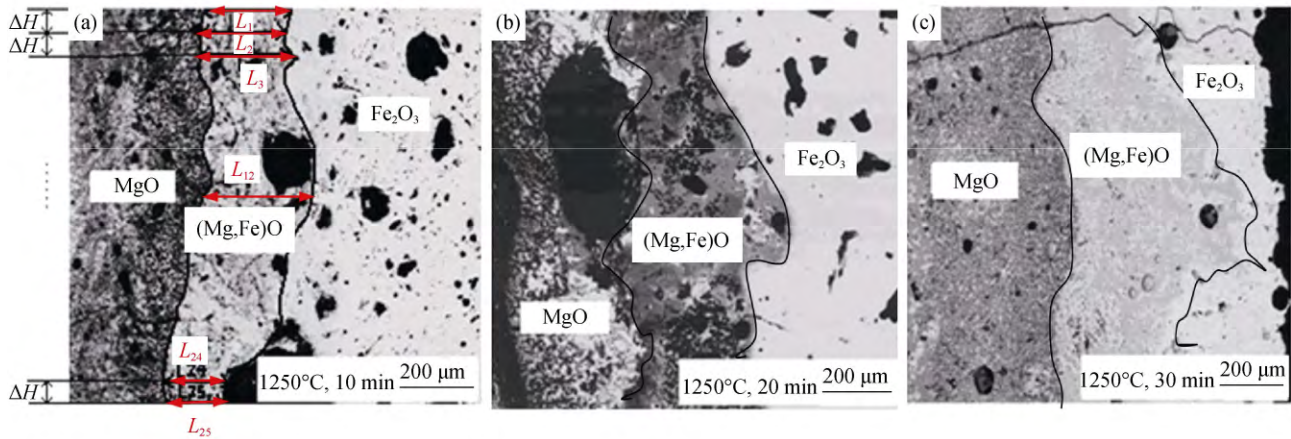


Fig. 5. Diffusion photographs of MgO–Fe<sub>2</sub>O<sub>3</sub> at a constant temperature of 1250°C over different time: (a) 10 min; (b) 20 min; (c) 30 min.

Table 2. Diffusion layer thickness

$t / \text{min}$	10	15	20	25	30
$L / \mu\text{m}$	225.5	292.1	367.1	433.3	498.3

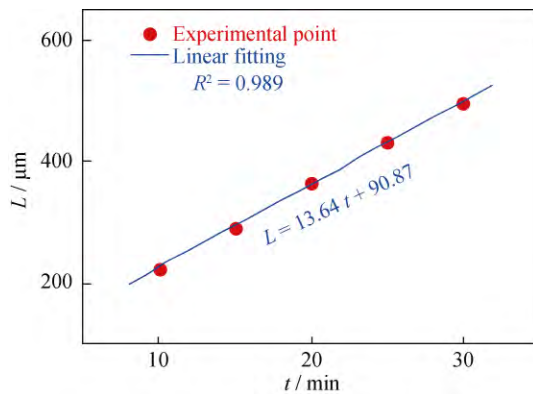


Fig. 6. Relationship between the diffusion layer thickness ( $L$ ) and time ( $t$ ).

$$v = dL/dt = 13.64 \mu\text{m}\cdot\text{min}^{-1} \quad (3)$$

Generally, the “–74  $\mu\text{m}$ ” proportion of iron ore concentrate makes up more than 80wt% of pellets. In other words, most iron ore particle size is less than 74  $\mu\text{m}$ . In the present work, the MgO diffusion rate was 13.64  $\mu\text{m}\cdot\text{min}^{-1}$ , which indicates that MgO can diffuse into 74  $\mu\text{m}$  iron ore particles over a period of 5 min. Actually, the induration time of pellets is much longer than 5 min and MgO diffuses into iron ore particles adequately under present pellet production methods.

## 4. Distribution and migration of MgO in MgO bearing pellets

### 4.1. Distribution of MgO in pellets

According to the MgO–Fe<sub>2</sub>O<sub>3</sub> diffusion experiments,

MgO can rapidly diffuse into the iron phase after just 5 min at 1250°C. The distribution of MgO was analyzed using pelletizing experiments and compared with acid pellets. The element distribution in the acid pellets is shown in Fig. 7. It can be found that the slag phase distributes independently from the iron phase. Si and O were discovered in slag phase.

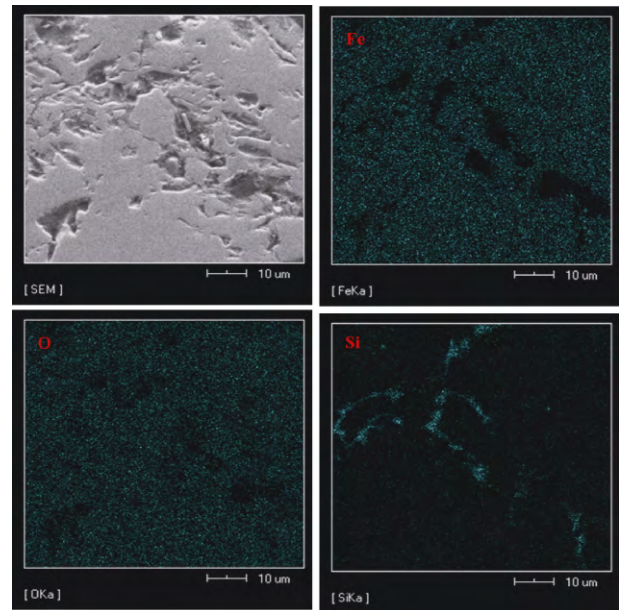


Fig. 7. SEM photograph and element distributions in ordinary acid pellets.

The SEM-EDX analysis of ordinary acid pellets is shown in Fig. 8. The atomic proportions of elemental Si and O indicate that the slag phase of the acid pellets is SiO<sub>2</sub>.

By comparison, the element distribution in the MgO-bearing pellets (4.0wt% MgO) is shown in Fig. 9. This suggests that most of the elemental Mg distributes uniformly

throughout the iron phase, which results in the generation of an MF phase. This is in good agreement with the diffusion experiment results. There is also a small amount of elemen-

tal Mg in the slag phase of the MgO-bearing pellets. The same as the acid pellets, the elemental Si and O distributes in the slag phase.

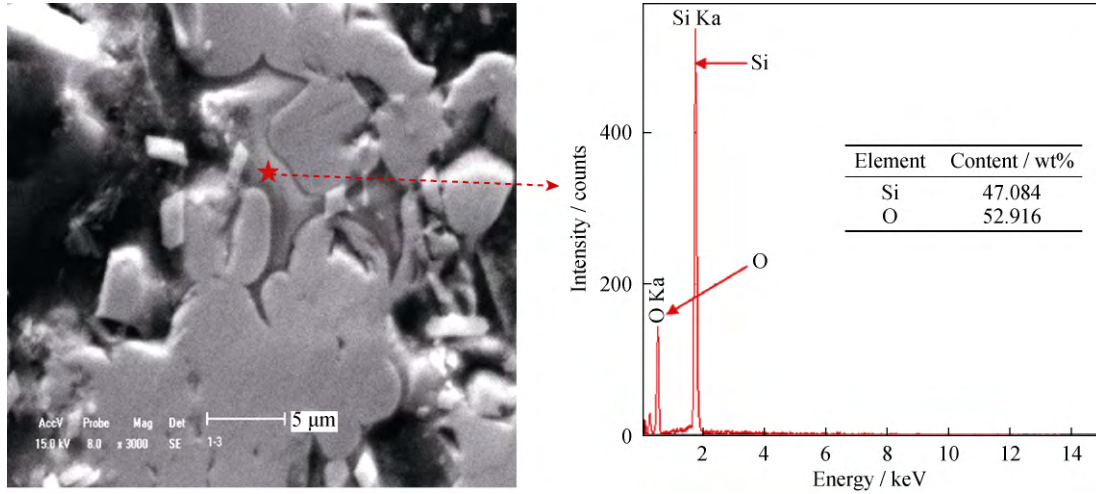


Fig. 8. SEM-EDX analysis results of ordinary acid pellets in the slag phase.

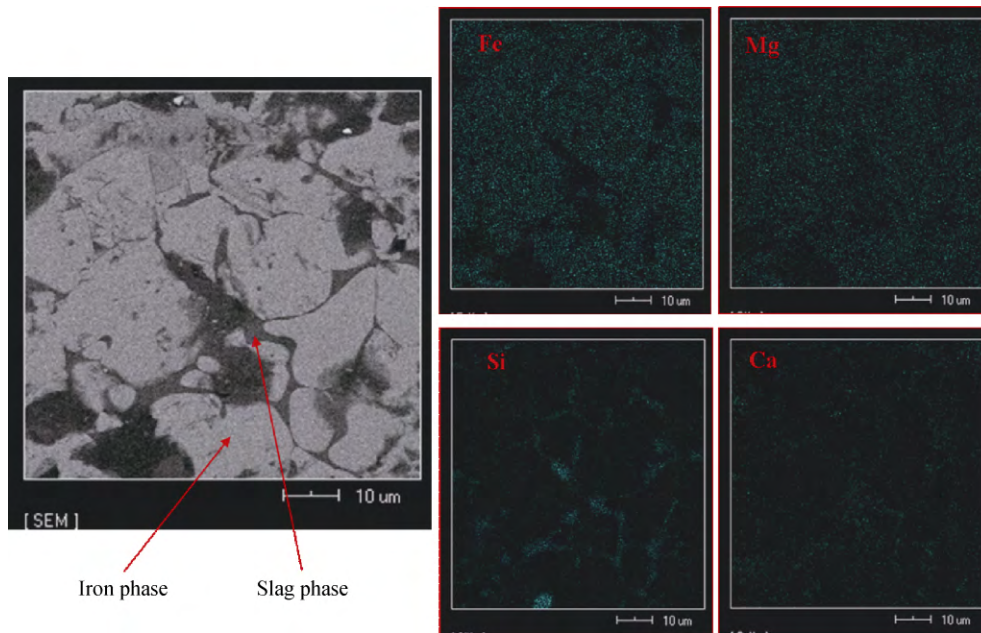


Fig. 9. SEM photograph and element distributions in MgO-bearing pellets.

#### 4.2. Distribution regulation of MgO in pellets

From the above analysis, it can be concluded that most of the MgO distributes in the iron phase rather than in the slag phase, and then an MF phase, is generated. In this work, we also discussed the distribution of MgO in a radial direction. The division for the radial directions of pellets is shown in Fig.10.

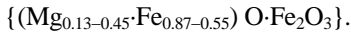
In order to facilitate comparison, the outer and inner layers of the iron phase of the MgO-bearing pellets were ana-

lyzed by SEM. Results are shown in Figs. 11 and 12, respectively, where differences in MgO distribution in the radial direction can be observed. The solid solution portion of MgO in the MF phase in the outer layer is larger than that in the inner layer. Based on the SEM-EDX analysis, the approximate chemical composition of the MF phase is calculated as follows.

MF phase in the pellet outer layer:



MF phase in the pellet inner layer:



## 5. Overall discussion

The generation of the MF phase in the pellets can be obtained from the fundamental theory of Mineralogy and Crystallography [23]. The radius of  $\text{Fe}^{2+}$  and  $\text{Mg}^{2+}$  are parallel ( $\text{Fe}^{2+}$ , 0.083 nm;  $\text{Mg}^{2+}$ , 0.078 nm), so they can replace each other and generate homogeneous phases. Additionally, from  $\text{FeO}_x\text{-MgO}$  phase diagrams [24], there is an unlimited mutual solution phenomenon between FeO and MgO shows that  $\text{Fe}^{2+}$  and  $\text{Mg}^{2+}$  can completely substitute for each other. There is a large homogeneous zone which coincides with the induration of oxidized pellets. So, during the induration process, the MF phase is produced.

To verify the above analysis, the mineral phase compositions of the ordinary acid pellets and MgO-bearing pellets were analyzed using XRD (Fig. 13). From this it can be seen

that the MF phase  $\{(\text{Mg}_{1-x}\text{Fe}_x)\text{O}\cdot\text{Fe}_2\text{O}_3\}$ ,  $x=0.36\}$  is found out in the MgO-bearing pellets, which is in agreement with the fundamental theories of Phase Diagrams and Mineralogy and Crystallography. Similarly, from the XRD analysis of the MgO-bearing and acid pellets,  $\text{SiO}_2$  appears (Fig. 13). This agrees well with the SEM-EDX results shown in Fig. 8.

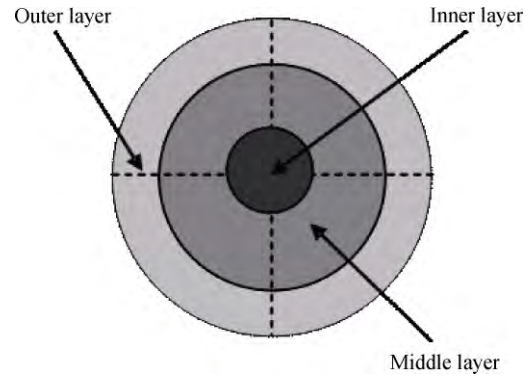


Fig. 10. Division of pellet layers

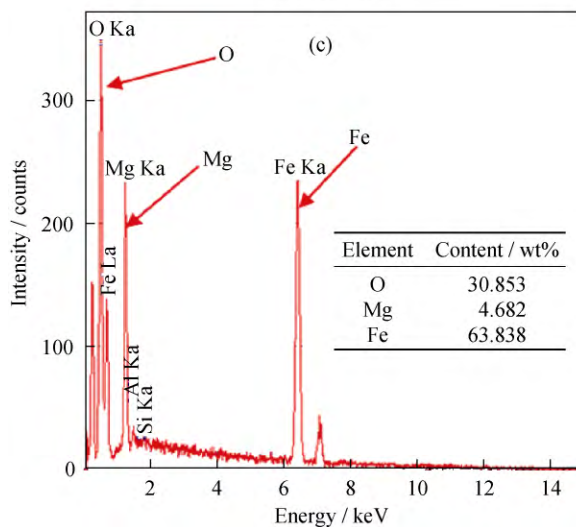
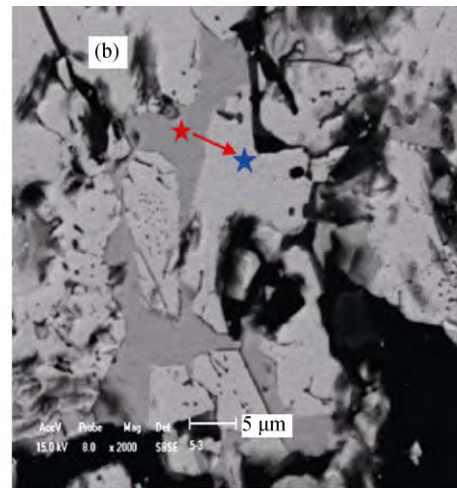
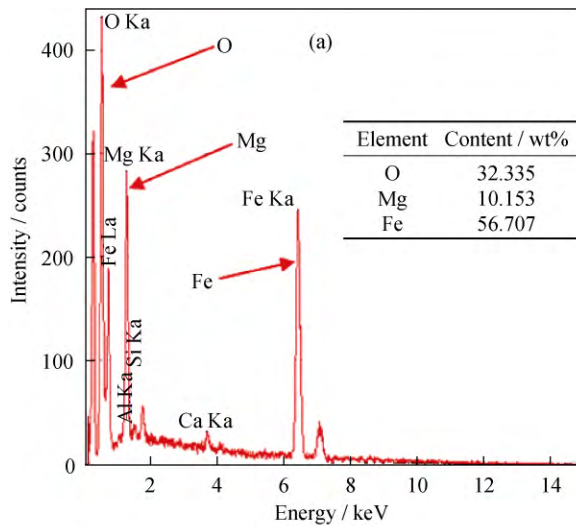


Fig. 11. Distribution of MgO in MF in the MgO-bearing pellet outer layer: (a) EDX analysis of point  $\star$ ; (b) SEM analysis of outer layer, (c) EDX analysis of point  $\star$ .

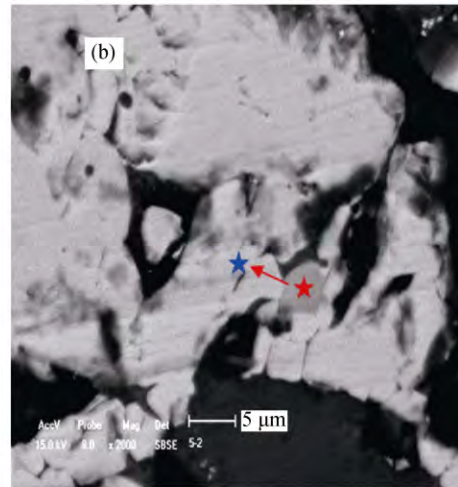
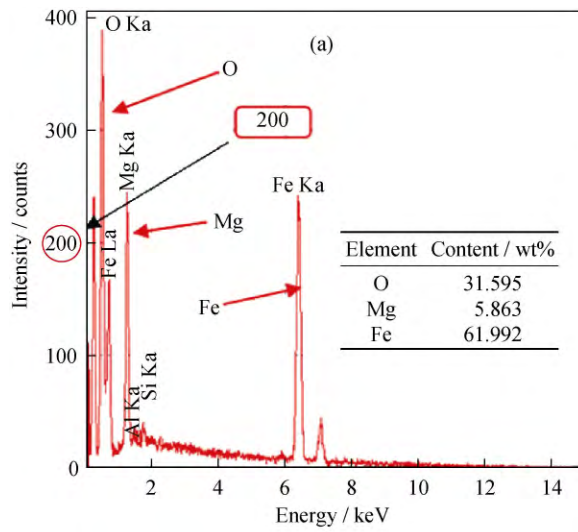


Fig. 12. Distribution of MgO in MF in the MgO-bearing pellet inner layer: (a) EDX analysis of point ★; (b) SEM analysis of the inner layer, (c) EDX analysis of point ★.

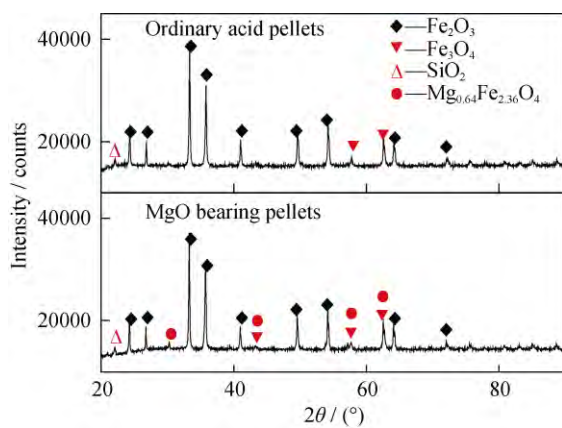
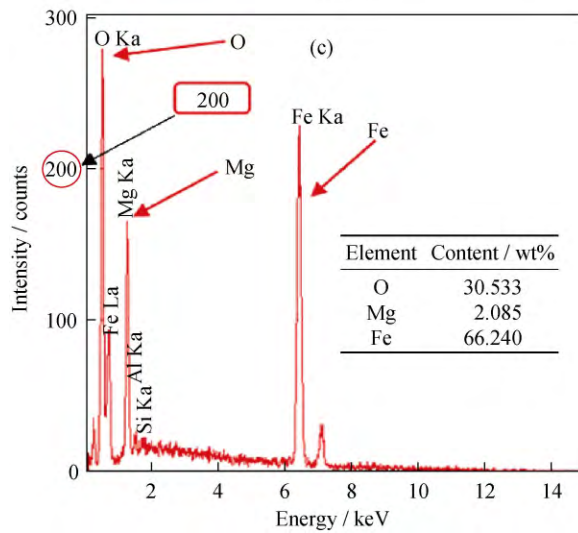


Fig. 13. XRD patterns of MgO-bearing pellets and ordinary acid pellets.

To summarize, MgO can rapidly diffuse and dissolve into Fe<sub>2</sub>O<sub>3</sub>; the diffusion rate can achieve 13.64 μm·min<sup>-1</sup>, which means that MgO can diffuse into 74 μm iron ore at 1250°C in just 5 min. Generally, the induration time of pellets

nowadays is much longer than 5 min, and adequate diffusion and reaction of MgO in pellets can be controlled for efficiency and economy by controlling the induration time.

## 6. Conclusions

In this work, the diffusion behavior of MgO in Fe<sub>2</sub>O<sub>3</sub> was investigated. The distribution and migration of MgO in pellets was analyzed. The main findings can be summarized as follows:

- (1) In the diffusion process between MgO and Fe<sub>2</sub>O<sub>3</sub>, MgO diffuses into Fe<sub>2</sub>O<sub>3</sub> by solid solution. The diffusion rate obtained in this experiment (heated from 900°C to 1250°C, then kept at 1250°C for 20 min) was 13.64 μm·min<sup>-1</sup>.
- (2) The slag phase is independent from iron phase in pellets. For the acid pellets, SiO<sub>2</sub> was present in the slag phase. In the MgO-bearing pellets, most of the MgO existed uniformly in the iron phase rather than in the slag phase, and

the MF phase was created.

(3) The distribution of MgO in the radial direction of the pellets was inconsistent. The solid solution proportion of MgO in the MF phase in the outer layer of the pellets was larger than in the inner layer. An approximate chemical composition of the MF phase, including the inner and outer pellet layers, is proposed.

## Acknowledgements

The authors would like to thank the editor and referees for their constructive comments and suggestions which have been used to improve the readability of the paper. Also, the financial support of China Postdoctoral Science Foundation (No. 2016M591445), Postdoctoral Science Foundation of NEU China (No. 20160302) and National Natural Science Foundation of China (No. 51604069) are much appreciated.

## References

- [1] F.M. Shen, Q.J. Gao, G. Wei, X. Jiang, and Y.S. Shen, Densification process of MgO bearing pellets, *Steel Res. Int.*, 86(2015), No. 6, p. 644.
- [2] J.Y. Fu and D.Q. Zhu, *Basic Principles, Techniques and Equipment of the Iron Ore Oxidized Pellets*, Central South University Press, Changsha, 2005, p. 336.
- [3] Q.J. Gao, F.M. Shen, X. Jiang, W. Guo, and H.Y. Zheng, Gas-solid reduction kinetic model of MgO-fluxed pellets, *Int. J. Miner. Metall. Mater.*, 21(2014), No. 1, p. 12.
- [4] T. Nishimura, K. Higuchi, M. Naito, and K. Kunitomo, Evaluation of softening, shrinking and melting reduction behavior of raw materials for blast furnace, *ISIJ Int.*, 51(2011), No. 8, p. 1316.
- [5] M. Iljana, O. Mattila, T. Alatarvas, J. Kurikkala, T. Paananen, and T. Fabritius, Effect of circulating elements on the dynamic reduction swelling behaviour of olivine and acid iron ore pellets under simulated blast furnace shaft conditions, *ISIJ Int.*, 53(2013), No. 3, p. 419.
- [6] T.J. Chun, D.Q. Zhu, and J. Pan, Influence of sulfur content in raw materials on oxidized pellets, *J. Cent. South Univ. Technol.*, 18(2011), No. 6, p. 1924.
- [7] S.H. Li, T.J. Chen, Y.M. Zhang, and J. Zhao, Experimental study on application of Mg-bearing additives in iron ore pellet, *Sintering Pelletizing*, 36(2011), No. 1, p. 33.
- [8] Q.J. Gao, G. Wei, X. Jiang, H.Y. Zheng, and F.M. Shen, Characteristics of calcined magnesite and its application in oxidized pellet production, *J. Iron Steel Res. Int.*, 21(2014), No. 4, p. 408.
- [9] G.F. Zhou and F. Yang, Effects of adding MgO on pelletizing ability and strength of pellet, *Res. Iron Steel*, 37(2009), No. 2, p. 10.
- [10] A. Kemppainen, O. Mattila, E.P. Heikkinen, T. Paananen, and T. Fabritius, Effect of H<sub>2</sub>-H<sub>2</sub>O on the reduction of olivine pellets in CO-CO<sub>2</sub> gas, *ISIJ Int.*, 52(2012), No. 11, p. 1973.
- [11] Q.J. Gao, G. Wei, Y.B. He, and F.M. Shen, Effect of MgO on compressive strength of pellet, *J. Northeast. Univ. Nat. Sci.*, 34(2013), No. 1, p. 103.
- [12] J. Pal, S. Ghorai, M.C. Goswami, D. Ghosh, D. Bandyopadhyay, and S. Ghosh, Behavior of fluxed lime iron oxide pellets in hot metal bath during melting and refining, *Int. J. Miner. Metall. Mater.*, 20(2013), No. 4, p. 329.
- [13] F.M. Shen, X. Jiang, G.S. Wu, G. Wei, X.G. Li, and Y.S. Shen, Proper MgO addition in blast furnace operation, *ISIJ Int.*, 46(2006), No. 1, p. 65.
- [14] Q.J. Gao, F.M. Shen, G. Wei, X. Jiang, and H.Y. Zheng, Effects of MgO containing additive on low-temperature metallurgical properties of oxidized pellet, *J. Iron Steel Res. Int.*, 20(2013), No. 7, p. 25.
- [15] A.K. Biswas, *Principles of Blast Furnace Ironmaking: Theory and Practice*, Cootha Publishing House, Brisbane, 1981, p. 38.
- [16] Q.J. Gao, Q.L. Wen, G. Wei, X. Jiang, and F.M. Shen, Study on the effect of caustic calcined magnesite to quality of green-pellets, [in] *The 4th Australia-China-Japan Symposium on Iron and Steelmaking*, Shengyang, 2012, p. 102.
- [17] J.V. Khaki, Y. Kashiwaya, and K. Ishii, High temperature behaviour of self-fluxed pellets during heating up reduction, *Ironmaking Steelmaking*, 21(1994), No. 1, p. 56.
- [18] X. Jiang, G.S. Wu, G.S. Li, and F.M. Shen, Study on improving the softening-melting properties of MgO bearing iron ores, *J. Northeast. Univ. Nat. Sci.*, 28(2007), No. 3, p. 365.
- [19] X. Wang, *Ferrous Metallurgy*, Metallurgical Industry Press, Beijing, 2002, p. 74.
- [20] P. Semberg, C. Andersson, and B. Björkman, Interaction between iron oxides and olivine in magnetite pellets during reduction to wustite at temperatures of 1000–1300°C, *ISIJ Int.*, 53(2013), No. 3, p. 391.
- [21] F.M. Shen, Q.J. Gao, X. Jiang, G. Wei, and H.Y. Zheng, Effect of magnesia on the compressive strength of pellets, *Int. J. Miner. Metall. Mater.*, 21(2014), No. 5, p. 431.
- [22] M. Singh and B. Björkman, Effect of reduction conditions on the swelling behaviour of cement-bonded briquettes, *ISIJ Int.*, 44(2004), No. 2, p. 294.
- [23] C.D. Zhou, *Technical Manual of Blast Furnace Production*, Metallurgical Industry Press, Beijing, 2002, p. 50.
- [24] V.D. Eisenhüttenleute, *Slag Atlas*, 2nd Ed., Verlag Stahleisen GmbH, Düsseldorf, 1995, p. 70.